Physica B 452 (2014) 37–41

Contents lists available at ScienceDirect

Physica B

journal homepage: www.elsevier.com/locate/physb

# Influence of Mn/Fe ratio on the magnetic properties of the $Mn_{2-x}Fe_xP_{0.5}As_{0.5}$, $0.5 \leq x \leq 1$ alloys

M. Budzyński [a], V.I. Valkov [b], A.V. Golovchan [b,c], V.I. Mitsiuk [d], A.P. Sivachenko [b], Z. Surowiec [a], T.M. Tkachenka [d,*]

[a] Institute of Physics, M. Curie-Sklodowska University, 1pl. M. Curie-Sklodowskiej, 20-031 Lublin, Poland
[b] Donetsk Institute for Physics and Engineering named after A.A. Galkin, NAS of Ukraine, 72 R. Luxemburg str., Donetsk 83114, Ukraine
[c] Donetsk National University, 24 Universitetskaya str., Donetsk 83001, Ukraine
[d] Scientific-Practical Materials Research Center of National Academy of Sciences of Belarus, 19 P. Brovky Str., Minsk 220072, Belarus

ARTICLE INFO

*Article history:*
Received 8 April 2014
Received in revised form
12 June 2014
Accepted 18 June 2014
Available online 9 July 2014

*Keywords:*
Magnetocaloric materials
Hyperfine magnetic field
Mössbauer spectroscopy

ABSTRACT

The analysis of 57Fe Mössbauer spectroscopy results for cation and anion substituted $Mn_{2-x}Fe_xP_{1-y}As_y$ was done in order to find out the influence of the Mn/Fe ratio on the magnetic properties of solid solutions and to compare experimental hyperfine parameters with those calculated from firstprinciples. The correlation between third Mössbauer sextet in $Mn_{2-x}Fe_xP_{0.5}As_{0.5}$ spectrum at 77K and stabilization of the antiferromagnetic phase for x = 0.5-0.6 was found on the basis of comparison between the magnetic phase diagrams and the "hyperfine field - iron content" dependence. The observed qualitative difference for $Mn_{2-x}FexP_{0.5}As_{0.5}$ and $MnFeAs_yP_{1-y}$ "hyperfine field - concentration" diagrams was interpreted on the basis of different mechanisms of magnetic phase stabilization and the different configurations of tetrahedral anionic environment of iron ions for systems with cation and anion substitutions.



## 1. Introduction

Materials demonstrating magnetocaloric effect are of rising interest now. The enhancement of magnetocaloric effect is usually accompanied by magnetic and magneto-structural phase transitions. The materials with the giant magnetocaloric effect near the room temperature are of special interest in the practical use [1–3]. Gd, $Mn_{2-x}Fe_xAs_yP_{1-y}$ alloys, MnAs-based alloys, NiMnGe and CoMnGe-based half-Heusler alloys etc. are referred to this group [4–9]. The $Mn_{2-x}Fe_xAs_yP_{1-y}$ solid solutions are supposed to be very promising ones because of possible practical applications [7–9]. The largest magnetocaloric effect ($\Delta S = -25$ J/kg K) is achieved for the materials in the vicinity of the first order phase transition from the paramagnetic state to the ferromagnetic one. This transition is accompanied by strong anisotropic magnetostriction with a weak change in the total volume. The latter significantly reduces hysteresis phenomena being especially important in practice.

The present work was aimed at the Mössbauer spectroscopy study of the effect of the Mn/Fe ratio on the magnetic properties of the $Mn_{2-x}Fe_xP_{0.5}As_{0.5}$ solid solutions and the comparison of experimental hyperfine parameters with those calculated from the first principles.

## 2. Experimental procedure

The powder samples of the $Mn_{2-x}Fe_xP_{0.5}As_{0.5}$ system with $x = 0.5$, 0.6, 0.7, 0.9 were synthesized by heating the appropriate mixtures of MnFeAs, MnFeP, $Mn_2As$, $Mn_2P$ at 1000 °C in evacuated silica tubes for 120 h [7–8]. After 72 h of subsequent treatment at 900 °C, the samples were slowly cooled to room temperature.

X-Ray diffraction (XRD) of the powder samples was performed at room temperature in DRON-3M diffractometer with Cu–Kα radiation, scan step was 0.03° , scan range was from 20° to 90° with 3 s exposition at every point. XRD patterns revealed that all samples were crystallized in the hexagonal crystal structure of $Fe_2P$ type (space group was $P\bar{6}2m$). According to the literature [9], at $x \leq 1$, the Fe and $Mn_I$ atoms occupied mainly the positions with tetrahedral environment of arsenic and phosphorus atoms ($I \equiv 3f$ ($x$, 0, 0) ); $Mn_{II}$ was associated with the pyramidal ($II \equiv 3g(x, 0, 1/2)$) one. The As and P atoms were randomly distributed at 2$c$ (1/3, 2/3, 0) and 1$b$ (0, 0, 1/2) positions, Fig. 1.

$^{57}$Fe Mössbauer spectra were recorded at 77 K and 300 K in standard transmission geometry using a constant acceleration

* Corresponding author. Tel.: +375 293283271; fax: +375 172840888.
*E-mail address:* lttt@physics.by (Z. Surowiec).

http://dx.doi.org/10.1016/j.physb.2014.06.042
0921-4526/

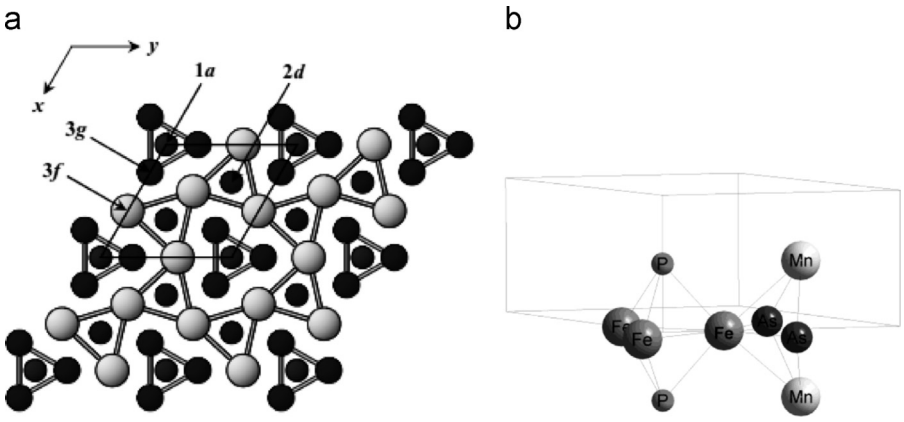


**Fig. 1.** Projection of the $Fe_2P$-type crystal structure along [0 0 1] direction (a), fragment of the $MnFeP_{0.5}As_{0.5}$ crystal structure (b).

mode spectrometer. The $^{57m}$Fe source embedded in a Rh matrix with a standart linewith of 0.11 mm/s was used.

The hyperfine fields $B_{\text{eff}}^{\text{calc}}$ were calculated with fully relativistic spin-polarized Korringa–Kohn–Rostoker method (SPRKKR program package [14]). The exchange–correlation potential energy was calculated within the generalized gradient approximation [15]. The crystal lattice potential was constructed within the atomic sphere approximation. Experimental lattice parameters [13] were used. The parameters of crystallographic positions for iron and manganese atoms were $x(3f)=0.257$ and $x(3\,g)=0.580$, respectively [9].

## 3. Results and discussion

### 3.1. $T=300$ K

The Mössbauer spectra of the hexagonal solid solutions $Mn_{2-x}Fe_xP_{0.5}As_{0.5}$ ($0.5 \le x \le 0.9$) at room temperature represent quadruple split doublets that correspond to the nonmagnetic states of samples at this temperature (Fig. 2, Table 1).

The absorption lines are slightly broadened. The isomer shifts (IS) of all spectra at room temperature practically coincide and have the value ~0.4 mm/s with respect to α-Fe, which corresponds to the shifts observed in $MnFeP_{1-x}As_x$ for $x=0.5$ [10–11]. The observed increase in isomer shift value at 77 K for all samples spectra is caused by the addition of the second-order Doppler shift (temperature shift). The quadruple splitting (QS) values are small and close in magnitude (~0.1 mm/s) for all samples, showing the stability of the coordination of the iron atoms. At the same time, the values of QS are insignificant, although the anionic environment of iron atoms does not have cubic symmetry. A similar fact has been found previously in $MnFeP_{0.5}As_{0.5}$ [10–11] as well as in the Fe–Mn alloys [12].

### 3.2. $T=77$ K

The Mössbauer spectra of the $Mn_{2-x}Fe_xP_{0.5}As_{0.5}$ at 77 K are shown in Fig. 3 and their parameters are listed in Table 2.

All samples show splitting which corresponds to their magnetic state [8]. The Mössbauer spectra of the samples with high iron content $x=0.7$ and 0.9 are well described by a superposition of two sextets with linewidth broadened with respect to the natural linewidth. Such spectrum model can be justified in terms of structure as follows. The Fe cation in the $MnFeP_{0.5}As_{0.5}$ ($x=1$) is in tetrahedral anionic enviroment (Fig. 1b). The interatomic distances (Table 3, [13]) comprise: $r$(Fe–As)=2.3083 Å, $r$(Fe–P)=2.3525 Å.

Usually the distribution of P and As atoms by anionic positions is equiprobable. Distances between the nearest metal atoms in $MnFeP_{0.5}As_{0.5}$ are: $r$(Fe–Fe)=2.7231 Å and $r$(Mn–Fe)=2.6395 Å, which is significantly greater than that for Fe–As and Fe–P. Thus, the hyperfine parameters of iron atom in the $MnFeP_{0.5}As_{0.5}$ ($x=1$) are mainly affected by two manganese and two iron atoms through anions. However, the Fe atoms in 3*f* positions in the $Mn_{2-x}Fe_xP_{0.5}As_{0.5}$ at a reduced iron content are replaced by manganese ones. Moreover, the manganese can replace one, two or none of the two iron ions that are the nearest to the fixed Fe ion. The realization of non-equivalent environments for the Fe ions results in different configurations of the $^{57}$Fe valence electrons in the Fe–As–Fe/Mn and Fe–P–Fe/Mn chains and appearance of two sextets in the spectrum. Each sextet corresponds to the positions of iron with slightly different values of the hyperfine magnetic fields at $^{57}$Fe ($B1_{\text{eff}}^{\text{exp}} \approx 20$ T and $B2_{\text{eff}}^{\text{exp}} \approx 18$ T). Iron content dependence of these quantities is presented in Fig. 4.

Deviation of the $M^{\text{exp}}(x)$ dependence starting at $x=0.7$ correlates with the deviation of the $H_{\text{eff}}^{\text{exp}}(x)$ function and indicates the existence of an intermediate state between pure AF and FM state. "X" corresponds to the saturation magnetic moment of magnetic field induced phase at $H=10$ T; vertical lines indicate the boundaries between the magnetically ordered phases.

Fig. 4 combined experimental (filled symbols) and calculated (open symbols) dependences $B_{\text{eff}}(x)$ and $M(x)$ (where $M$ is the magnetic moment of the atom). Experimental $M_{\text{exp}}(x)$ dependences were obtained in Ref. [13] and were qualitatively similar to our experimental $B_{\text{eff}}^{\text{exp}}(x)$ dependences. Theoretical dependences $M_{\text{FM}}^{\text{calc}}(x)$, $B_{\text{eff}}^{\text{calc}}(x)$ for FM phase are calculated from first-principles by SPRKKR programm [14]. According to Fig. 4, the correlation between experimental $M^{\text{exp}}(x)$ and calculated $M_{\text{FM}}^{\text{calc}}(x)$ is observed mainly in concentration region $0.7 \le x \le 1.0$. At further decrease of iron content, the dependencies diverge, separating the FM region from the region of FM and AF coexistence ($0.5 < x < 0.7$) and from the region of stable AF-state of the sample ($x \le 0.5$) [13]. The experimental $B_{\text{eff}}^{\text{exp}}(x)$ and calculated from first principles $B_{\text{eff}}^{\text{calc}}(x)$ hyperfine magnetic field values are in general agreement with this phase diagram. As follows from Fig. 4, the behavior of genetically close dependences $B1_{\text{eff}}^{\text{exp}}(x)$ and $B2_{\text{eff}}^{\text{exp}}(x)$ coincides with the behavior of the $M^{\text{exp}}$(x). Indeed, in the region of FM-state stability ($0.5 < x < 0.7$), the hyperfine field values $B1_{\text{eff}}^{\text{exp}}(x)$, $B2_{\text{eff}}^{\text{exp}}(x)$ increase at iron content increasing as well as $M^{\text{exp}}$(x).

For $x < 0.7$ ($x=0.5$, 0.6) the qualitative changes occur in the Mössbauer spectrum of $Mn_{2-x}Fe_xP_{0.5}As_{0.5}$ [16]. The spectra of the samples at 77 K represent the superposition of three sextets and two singlets (Table 2, Fig. 2). As a consequence, the emergence of the third component of hyperfine field $B3_{\text{eff}}^{\text{exp}}$ and a significant

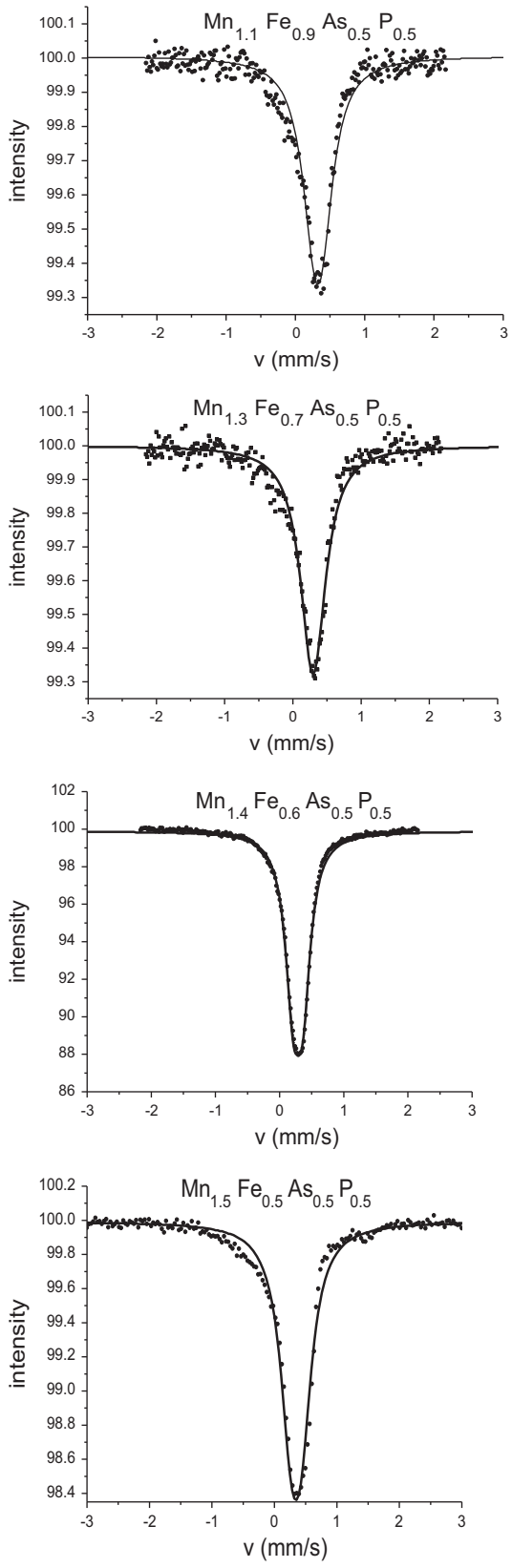


**Fig. 2.** The $^{57}$Fe Mossbauer spectra of hexagonal $Mn_{2-x}Fe_xP_{0.5}As_{0.5}$ solid solutions at room temperature.

reduction of other components takes place. The slopes of $B1^{exp}_{eff}(x)$, $B2^{exp}_{eff}(x)$, $B3^{exp}_{eff}(x)$ (Fig. 4) are changed, being consistent with the corresponding changes in the magnetization ($M^{exp}$) due to initiation of antiferromagnetic contribution to the total magnetic moment of the system [13]. At the same time, dependences $B^{calc}_{eff}(x)$, $M^{calc}_{FM}(x)$, if calculated for FM-state, do not show abnormal changes in the range of iron content under the study.

**Table 1**
The Mössbauer spectra parameters for $Mn_{2-x}Fe_xP_{0.5}As_{0.5}$ at $T=300$ K.

| Sample | IS (mm/s) | QS (mm/s) | $\Gamma$ (mm/s) |
|---|---|---|---|
| $Mn_{1.1}Fe_{0.9}As_{0.5}P_{0.5}$ | 0.32 | 0.12 | 0.21 |
| $Mn_{1.3}Fe_{0.7}As_{0.5}P_{0.5}$ | 0.29 | 0.08 | 0.21 |
| $Mn_{1.4}Fe_{0.6}As_{0.5}P_{0.5}$ | 0.29 | 0.15 | 0.14 |
| $Mn_{1.5}Fe_{0.5}As_{0.5}P_{0.5}$ | 0.36 | 0.18 | 0.19 |

The agreement of the anomalous behavior of the magnetic ($M^{exp}(x)$) and Mössbauer ($B1^{exp}_{eff}(x)$, $B2^{exp}_{eff}(x)$, $B3^{exp}_{eff}(x)$) characteristics as well as the emergence of the third sextet in the Mössbauer spectrum may be conditioned by the appearance of interacting spin–density waves in the 3d-electronic subsystem of iron and manganese atoms situated in 3*f* positions [10].

In truth the origination of spin–density wave is associated with the stabilization of the electronic states. The states at local centers discern not only by the angle of magnetic moments, but also by their modulus [10]. In other words, at cationic substitution, the appearance of antiferromagnetic contributions to the total magnetic moments corresponds to the appearance of additional $^{57}$Fe environment configurations, where the absolute magnitudes of the local iron and manganese magnetic moments are different.

In the $MnFeAs_yP_{1-y}$ system, the Mn and Fe ions occupy different crystallographic positions (notably 3*g* for Mn and 3*f* for Fe). There is a lack of varying of 3d-electron configurations in iron environment. The result is a single sextet structure of Mössbauer spectra. The hyperfine field concentration dependence $B^{exp}_{eff}(y)$ qualitatively differs from $B^{exp}_{eff}(x)$ (Fig. 5) because of the interchange of magnetically ordered phases in $MnFeAs_yP_{1-y}$. According to Ref. [13] and Fig. 5, the FM state in $MnFeAs_yP_{1-y}$ system can be observed in the whole range of the arsenic content. However, if $y=0.35$, a high-temperature AF state precedes a low-temperature FM, then FM state becomes metastable at $y=0.2$ and does not occur spontaneously. It can occur only as a result of the irreversible first-order AF–FM transition induced by magnetic field [13]. In contrast to the $Mn_{2-x}Fe_xP_{0.5}As_{0.5}$ system, the magnetic field induced state at $y=0.2$ in $MnFeAs_yP_{1-y}$ is a pure FM state since the magnetic moment of induced irreversible phase is not less than the magnetic moment of the stable FM-state ($y>0.35$). This fact is also confirmed by the calculated values of hyperfine fields $B^{calc}_{eff}(y)$ for FM-state, which are in reasonable agreement with the experimental $B^{exp}_{eff}(y)$, Fig. 5.

The vertical arrows indicate the possible AF–FM phase transitions induced by temperature or magnetic field.

Thus, in the $MnFeAs_yP_{1-y}$ system for $y\leq 0.35$ the pure FM or pure AF states can be observed (at different external actions, namely, temperature, magnetic field). The absence of the intermediate magnetic moment values for spontaneous ($y\geq 0.35$) and induced ($y<0.35$) states in this case correlates with the $B^{exp}_{eff}(y)$ behavior.

The dependence of the single hyperfine field value $B^{exp}_{eff}(y)$, Fig. 5, at $y=0.35$ undergoes a kink from $B^{exp}_{eff}(FM)=18.6$ T to $B^{exp}_{eff}(AF)=10$ T [11]. Thus, the difference between $B^{exp}_{eff}(FM)$ and $B^{exp}_{eff}(AF)$ at $y\leq 0.35$ is constant. For the AF-state of the sample, the Mössbauer spectrum is described by one sextet corresponding to the one hyperfine field value at Fe [11].

It is interesting to compare the Mössbauer results obtained and the temperature dependence of the isothermal magnetic entropy ([8], Fig. 6).

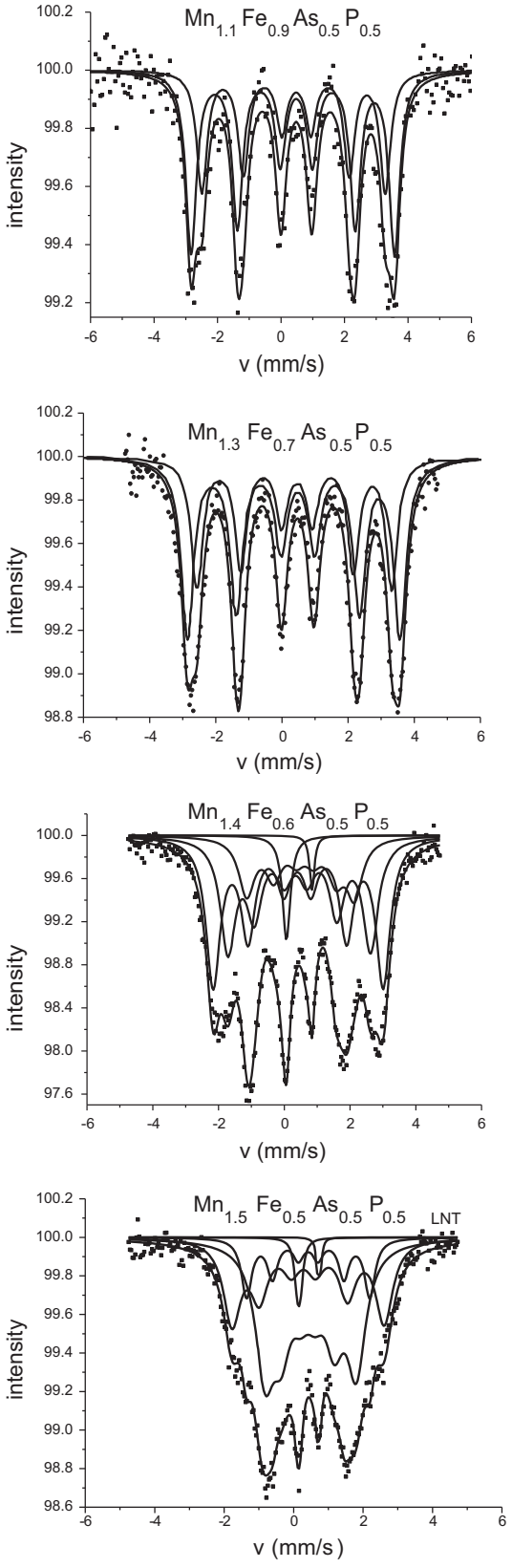


**Fig. 3.** The $^{57}$Fe Mossbauer spectra of the $Mn_{2-x}Fe_xP_{0.5}As_{0.5}$ hexagonal solid solutions at 77 K.

The best magnetocaloric properties of the $Mn_{2-x}Fe_xP_{0.5}As_{0.5}$ are found at $x=0.9$ (peak of the $\Delta S$ (T) dependence, Fig. 6), that are significantly reduced at $x=0.7$ and 0.6. In terms of Mössbauer and magnetic data obtained, one of the reasons causing the degradation of magneto-caloric properties could be the reduction of FM contribution to the magnetic moment of the system and also the presence of non-magnetic phases in the sample that have not been detected by X-ray analysis. Mössbauer spectroscopy having extremely high sensitivity allows fixation of the impurity phase even in small quantities.

**Table 2**
$^{57}$Fe Mossbauer spectra parameters for $Mn_{2-x}Fe_xP_{0.5}As_{0.5}$ at $T=77$ K.
* – The characteristics calculated for FM state with SPRKKR package [14].

| Sample, $x$ | No. sub spectra | IS (mm/s) | QS (mm/s) | $B_{eff}^{exp}$ (T) | $\Gamma$ (mm/s) | $A$ (%) | $*B_{eff}^{calc}$ FM (T) | $*\mu_{FM}^{calc}(3f)$ $\mu(Fe_{3f})$ ($\mu_B$) |
|---|---|---|---|---|---|---|---|---|
| 0.4 | 1 | | | | | | 16.1 | 1.62 |
| 0.5 | 1 | 0.35 | 0.08 | 13.6 | 0.29 | 30 | 16.65 | 1.6 |
| | 2 | 0.42 | 0.02 | 11 | 0.17 | 13 | | |
| | 3 | 0.45 | 0.04 | 8.2 | 0.32 | 53 | | |
| | 4 | 0.15 | – | – | 0.12 | 2.8 | | |
| | 5 | 0.73 | – | – | 0.10 | 1.1 | | |
| 0.6 | 1 | 0.41 | 0.01 | 16.1 | 0.26 | 35 | 16.71 | 1.57 |
| | 2 | 0.40 | 0.05 | 13.5 | 0.28 | 38.7 | | |
| | 3 | 0.56 | −0.04 | 10.2 | 0.29 | 20.9 | | |
| | 4 | 0.06 | – | – | 0.11 | 4 | | |
| | 5 | 0.81 | – | – | 0.099 | 1.3 | | |
| 0.7 | 1 | 0.42 | −0.06 | 19.9 | 0.22 | 59.8 | 16.57 | 1.52 |
| | 2 | 0.42 | −0.04 | 18.3 | 0.20 | 40.2 | | |
| 0.8 | | | | | | | 16.68 | |
| 0.9 | 1 | 0.41 | −0.05 | 19.9 | 0.19 | 60.3 | 16.76 | |
| | 2 | 0.42 | −0.04 | 17.9 | 0.19 | 39.7 | | |
| 1.0 | | | | | | | 16.97 | 1.42–1.46 |

**Table 3**
Interatomic distances in $MnFeP_{0.5}As_{0.5}$.

| N | Atom 1 | Atom 2 | Distance (Å) |
|---|---|---|---|
| 1 | P | Fe | 2.3525 |
| 2 | P | Mn | 2.5694 |
| 3 | Mn | Fe | 2.6395 |
| 4 | Mn | As | 2.5339 |
| 5 | Fe | Fe | 2.7231 |
| 6 | Fe | As | 2.3084 |
| 7 | Mn | Fe | 2.6395 |

## 4. Conclusion

Mössbauer data allowed detection of two stable configurations of the local iron atom environments realized in the ferromagnetic phase in $Mn_{2-x}Fe_xP_{0.5}As_{0.5}$ at $0.7 \le x \le 0.9$. These configurations correspond to two sextets in Mössbauer spectrum with hyperfine magnetic field values $B2_{eff}^{exp} < B1_{eff}^{exp}$ at $^{57}$Fe nuclei. At iron concentrations $0.5 \le x < 0.7$ the Mössbauer spectrum of the $Mn_{2-x}Fe_xP_{0.5}As_{0.5}$ changes from two sextets superposition to that of three sextets. All corresponding field values are reduced and related as $B3_{eff}^{exp} < B2_{eff}^{exp} < B1_{eff}^{exp}$. The abnormal change of the Mössbauer characteristics for $x < 0.7$ is correlated with the changes of the magnetic moment of the system and determined by the nature of antiferromagnetic structure formation in transition metal sublattices. The qualitative difference between the "hyperfine field-concentration" diagrams for the $Mn_{2-x}Fe_xP_{0.5}As_{0.5}$ systems with

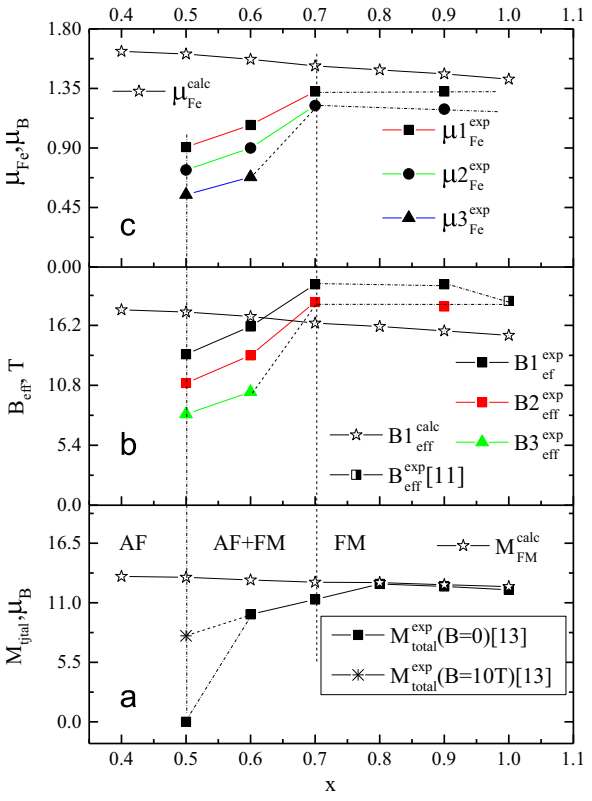


**Fig. 4.** Iron content dependence of experimental (filled symbols) and calculated (open symbols) values of the total magnetic moment and the hyperfine magnetic field in the $Mn_{2-x}Fe_xP_{0.5}As_{0.5}$ system.

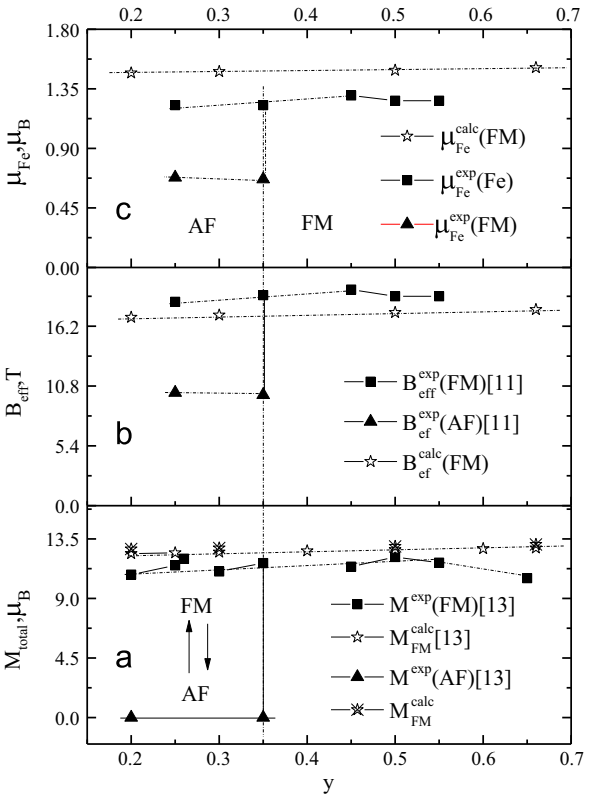


**Fig. 5.** The dependence of experimental (filled symbols) and calculated (open symbols) values of the total magnetic moment and hyperfine field on the As-concentration in the $MnFeAs_yP_{1-y}$ system.

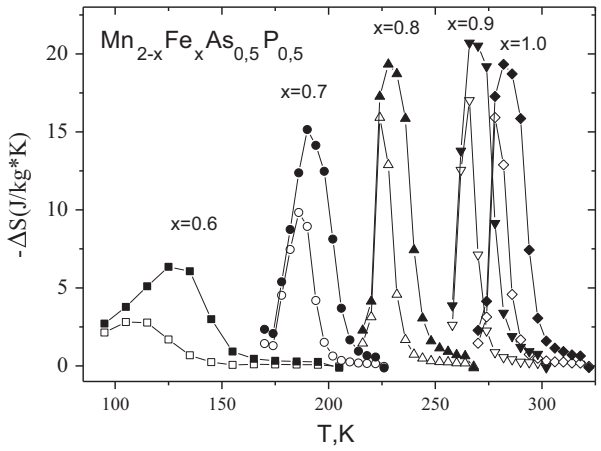


**Fig. 6.** The temperature dependences of the changes of isothermal magnetic entropy for $Mn_{2-x}Fe_xP_{0.5}As_{0.5}$ alloys at magnetic field values from 0 to 2 T (open symbols) and from 0 to 4 T (filled symbols).

cationic substitutions (Fig. 4) and $MnFeAs_yP_{1-y}$ with anionic ones (Fig. 5) is caused by dramatic differences in the mechanism of stabilization of magnetically ordered phases and the differences in the configuration environment of iron ions in 3*f*-positions.

## Acknowledgments

The work was supported in part by Grant no. T13K-003 (Belarusian Republican Foundation for Fundamental Research) and No. Φ54.1/003 (Ukrainian Foundation for Fundamental Research).

## References

[1] A.M. Tishin, Y.I. Spichkin, The magnetocaloric effect and its applications, IOP Publishing, Bristol, Philadelphia, 2003.
[2] K.A. Gschneider, V.K. Pecharsky, A. Tsokol, Rep. Progr. Phys. 68 (2005) 1479.
[3] K.A. Gschneidner, V.K. Pecharsky, Int. J. Refrig. 31 (2008) 945.
[4] K.A. Gschneidner, Acta Mater. 57 (2009) 18.
[5] E. Brück, O. Tegus, D.T. Cam Thanh, Nguyen T. Trung, K.H.J. Buschow, Int. J. Refrig. 31 (2008) 763.
[6] E Brück, O Tegus, X.W Li, F.R. de Boer, K.H.J. Buschow, Physica B 327 (2003) 431.
[7] V.I. Valkov, D.V. Varyukhin, A.V. Golovchan, Low Temp. Phys. 34 (2008) 427.
[8] I.F. Gribanov, A.V. Golovchan, D.V. Varyukhin, et al., Low Temp. Phys. 35 (2009) 786.
[9] R. Zach, B Malaman, M Bacmann, et al., J. Magn. Magn. Mater. 147 (1995) 201.
[10] B. Malaman, G.L. Caer, P. Delcroix, et al., J. Phys.: Condens. Matter 8 (1996) 8653.
[11] Raphael P. Hermann, O. Tegus, et al., Phys. Rev. B 70 (2004) 214425-1.
[12] G.K. Wertheim, Int. Atomic Energy Agency (1966).
[13] V.I. Val'kov, A.V. Golovchan, D.V. Varyukhin, et al., J. Magn. Magn. Mater. 324 (2012) 3043.
[14] H. Ebert, D. Kodderitzsch, J. Minar, Rep. Prog. Phys. 74 (2011) 096501 http://dx.doi.org/10.1088/0034-4885/74/9/096501 (H. Ebert et al. The Munich SPR-KKR package, version 6.3) ⟨http://ebert.cup.uni-muenchen.de/SPRKKR⟩.
[15] J.P. Perdew, K. Burke, M. Ernzerhof, Phys. Rev. Lett. 77 (1996) 3865.
[16] V.I. Mitsiuk, T.M. Tkachenka, M. Budzyński, Z. Surowiec, V.I. Valkov, Nukleonika 58 (2013) 169.